

Regenerative Potential of Fibroblast Secretome: Keratinocyte Growth Factor (KGF) and Total Protein Effects on Senescent Cell Proliferation via Mek 1/2 Activation and Enhanced Collagen Type 1 Utilization



Marisa Riliani^{1,*}, Endang Purwaningsih¹, Himmi Marsiati¹, Indra Kusuma¹, Diniwati Mukhtar¹, Restu Syamsul Hadi¹ and Rilianawati²

¹Doctoral Program in Biomedical Sciences, YARSI University, Menara Yarsi, Jl. Letjen Suprpto No.Kav.13, RT.10/RW.5, Cempaka Putih Timur, Jakarta, 10510, Indonesia

²Center for Vaccine and Drug Research, National Research and Innovation Agency, KST BJ Habibie, Tangerang Selatan, West Java, 15314, Indonesia

Abstract:

Introduction: Aging leads to reduced physical, mental, and social performance, lowering productivity. The fibroblast secretome, rich in bioactive proteins, growth factors, and enzymes, is essential for cell repair and regeneration. This study evaluated its regenerative potential by examining MEK1/2 pathway activation and type I collagen utilization to enhance senescent fibroblast proliferation.

Methods: Young (passage 3) and senescent (passage 24) fibroblasts were cultured in DMEM. Senescent cells were treated with 10% or 20% fibroblast secretome. Culture media were collected on days 1, 3, 5, and 7 for analysis of total protein, KGF, cell proliferation, MEK phosphorylation, and collagen concentration.

Results: The 20% secretome contained $5830,67 \pm 181,62$ $\mu\text{g/mL}$ total protein and $1712,67 \pm 7,19$ pg/mL KGF. Senescent fibroblasts treated with 20% secretome showed a 44% proliferation increase on day 5 ($21135,67 \pm 1392,89$ cells/well) versus controls ($14637 \pm 2250,57$ cells/well, $p < 0,05$). MEK1/2 phosphorylation rose from $0,01 \pm 0,00$ pg/mL at 45 minutes to $0,18 \pm 0,03$ pg/mL at 24 hours ($p < 0,05$), indicating sustained activation.

Discussion: Secretome treatment enhanced MEK1/2 signaling and proliferation, with a 12% reduction in extracellular type I collagen on day 5 ($2,67 \pm 0,03$ ng/mL vs. $3,02 \pm 0,03$ ng/mL , $p < 0,05$), reflecting increased collagen utilization and matrix remodeling.

Conclusion: The 20% fibroblast secretome enriched with KGF and bioactive proteins promotes senescent fibroblast proliferation via MEK1/2 activation and optimized collagen dynamics, supporting its potential in regenerative medicine for aging and tissue repair.

Keywords: Secretome, Senescent cell proliferation, Total protein, KGF, MEK 1/2, Collagen type 1.

© 2026 The Author(s). Published by Bentham Open.

This is an open access article distributed under the terms of the Creative Commons Attribution 4.0 International Public License (CC-BY 4.0), a copy of which is available at: <https://creativecommons.org/licenses/by/4.0/legalcode>. This license permits unrestricted use, distribution, and reproduction in any medium, provided the original author and source are credited.

*Address correspondence to this author at the Doctoral Program in Biomedical Sciences, YARSI University, Menara Yarsi, Jl. Letjen Suprpto No.Kav.13, RT.10/RW.5, Cempaka Putih Timur, Jakarta, 10510, Indonesia; E-mail: marisa.riliani@yarsi.ac.id

Cite as: Riliani M, Purwaningsih E, Marsiati H, Kusuma I, Mukhtar D, Hadi R, Rilianawati. Regenerative Potential of Fibroblast Secretome: Keratinocyte Growth Factor (KGF) and Total Protein Effects on Senescent Cell Proliferation via Mek 1/2 Activation and Enhanced Collagen Type 1 Utilization. Open Biotechnol J. 2026; 20: e18740707430933. <http://dx.doi.org/10.2174/0118740707430933251216071858>



Received: August 26, 2025
Revised: October 21, 2025
Accepted: November 03, 2025
Published: March 02, 2026



Send Orders for Reprints to
reprints@benthamscience.net

1. INTRODUCTION

Aging is a natural process that occurs in every living creature and is marked by a decline in physical, mental, and social abilities. Aging can occur earlier than one's chronological age, which significantly affects a person's productivity in daily life. In 2020, the population aged 60 years exceeded the population aged 5 years. Between 2015 and 2050, the population aged 60 years will increase twofold from 12% to 22%. By 2050, it is estimated that the elderly population in middle and lower-income countries will reach 80%. With a longer life, one has opportunities to remain active, such as opportunities for education, work, and socialization. However, all these opportunities depend on one factor: health. If this change in the elderly population's proportion is accompanied by poor health, the implications will be severe [1]. Extrinsic and intrinsic factors cause the aging process at the cellular level. Extrinsic aging factors can result from pollution and unhealthy lifestyles. Meanwhile, intrinsic factors can be caused by hormones, free radicals, genetic instability, and the formation of senescent cells. During human development, the number of senescent cells remains small compared to healthy cells, so the body's physiological processes continue to function well. At a certain threshold, the number of senescent cells becomes more dominant, and diseases caused by this aging process will emerge [2].

Secretome refers to all organic and inorganic molecules secreted by a cell into the extracellular space. These molecules include growth factors, free nucleic acids, lipids, extracellular vesicles, enzymes, cytokines, chemokines, interferons, colony-stimulating factors (CSFs), and tumor necrosis factors (TNFs). The fibroblast secretome, rich in various proteins, genetic material, growth factors, and enzymes, is expected to enhance cellular responses during the regeneration process. The use of secretome for regenerative treatment has increased rapidly because it is a cell-free therapy, thereby avoiding immune compatibility issues, tumorigenicity, and the transmission of infections. Additionally, secretomes can be stored for a long time and mass-produced [3]. Growth factors are needed for cell growth; one is Keratinocyte Growth Factor (KGF). KGF is part of the Fibroblast Growth Factor Family (FGF-7) that has potential mitogenic activity. KGF protein transcription is observed in almost all mesenchymal and stromal cells, particularly dermal fibroblasts, but epithelial cells do not produce KGF. Epithelial cells only have KGF receptors, so the growth and differentiation of epithelial cells are partly a result of paracrine induction from KGF produced by fibroblast cells. KGF will bind to receptors on epithelial cells, namely tyrosine kinase receptor (FGFR2-IIIb/KGFR), which will induce the Ras-mitogen-activated protein kinase (Ras/MAPK) cascade pathway and phosphoinositide 3-kinase-Akt (PI3K/AKT) [4].

Mitogen-activated protein (MAP) kinases are pivotal protein kinases in eukaryotic signal transduction that govern cell growth and differentiation. One key MAP kinase, extracellular signal-regulated kinase (ERK), is activated *via* a two-step kinase cascade: RAS activates

RAF, a serine/threonine kinase that phosphorylates and activates MEK1/2, a dual-specificity mitogen-activated protein kinase kinase (MAPKK). MEK1/2 specifically phosphorylates ERK on threonine and tyrosine residues, triggering downstream phosphorylation of other kinases and transcription factors that regulate cellular processes such as metabolism, cell cycle progression, proliferation, migration, differentiation, and apoptosis. MEK1/2 functions as a critical signaling node, with regulatory domains that tightly control kinase activity, thereby maintaining cellular homeostasis and preventing aberrant signaling associated with pathological states. In fibroblasts, this MEK/ERK cascade plays a central role in modulating proliferation, survival, and Extracellular Matrix (ECM) remodeling [5].

Mitogen-Activated Protein (MAP) kinase is a type of protein kinase that has a central role in signal transduction in eukaryotic cells and is a major pathway for cell growth and differentiation. One form of MAP kinase is extracellular signal-regulated kinase (ERK). ERK action is mediated by 2 types of protein kinases. The first is RAS, which activates the Raf protein-serine/threonine kinase, resulting in the phosphorylation and activation of the second protein kinase, MEK1/2, which is one of the mitogen-activated protein kinase kinase (MAPKK) pathway proteins. MEK 1/2 will phosphorylate threonine and tyrosine of ERK, so ERK will be activated to phosphorylate other protein kinases and gene transcription factors (Elk-1, c-Fos, c-Jun (AP-1 complex), CREB, ATF2, and Myc), allowing cells to perform functions such as metabolism, cell cycle, proliferation, migration, differentiation, or apoptosis [6]. Collagen plays an important role in the shape of fibroblast cells and mechanical pressure in various tissues. In the young dermis layer, the bond between fibroblast cells and collagen fibrils is very tight, maintaining the shape and size of fibroblast cells and the firmness of skin tissue. In the elderly dermis, collagen fibril bonds are reduced, causing fibroblast cells to shrink in size and shape [7]. Collagen is an Extracellular Matrix (ECM) protein that controls cell survival, proliferation, migration, and differentiation. In *in vitro* studies, collagen is used to increase cell adhesion to the cell culture surface. Collagen significantly promotes cell proliferation, resulting in short doubling times. Additionally, the collagen matrix efficiently protects cells from oxidative stress-induced cell death. Cell attachment to collagen is also high and occurs rapidly; therefore, culturing cells on collagen will help achieve high cell proliferation and survival [8].

The MEK1/2-ERK1/2 signaling pathway plays a central role in regulating fibroblast and keratinocyte functions, including proliferation, survival, and extracellular matrix remodeling, which are critical for tissue repair and regeneration. Activation of MEK1/2 by growth factors such as Keratinocyte Growth Factor (KGF) triggers phosphorylation cascades that modulate transcription factors and cell cycle proteins, promoting fibroblast activation and reversing cellular senescence. Recent studies highlight MEK1/2 involvement in rejuvenating

aged fibroblasts and enhancing collagen type-1 utilization, supporting its mechanistic role in regenerative processes. KGF, a specific fibroblast-derived mitogen, activates MEK1/2 signaling more directly and potently than the total protein content of the secretome, which represents a complex mixture of bioactive molecules. Therefore, comparing the effects of KGF *versus* total protein allows clarification of whether regenerative outcomes are driven by key growth factors through defined signaling pathways or by the collective action of multiple secretome components. This distinction is essential for understanding the molecular basis of fibroblast-secretome-mediated regeneration and for optimizing therapeutic strategies targeting aging and tissue repair [9].

Despite growing evidence supporting the roles of fibroblast secretome and MEK/ERK signaling in aging and regeneration, the precise mechanisms by which fibroblast secretome influences MEK1/2 activation and collagen utilization in senescent cells remain unclear. Most studies have focused on individual growth factors or cell-based approaches, leaving a knowledge gap regarding the combined effects of the complex secretome mixture on these pathways. Furthermore, it is not fully understood whether key factors, such as KGF alone, drive regenerative responses or whether the synergistic action of multiple secretome components is necessary.

This study aims to elucidate the mechanistic role of fibroblast secretome in reversing cellular senescence, particularly by examining its effects on MEK1/2 signaling pathway activation and type-1 collagen utilization in senescent fibroblast cells. We hypothesize that the secretome's regenerative effects on senescent fibroblast proliferation are mediated through these specific molecular pathways. Understanding these underlying mechanisms will provide critical guidance for developing optimized secretome-based therapies for age-related degenerative conditions.

2. MATERIALS AND METHODS

2.1. Study Design

The study design is experimental, with a qualitative approach to data collection and analysis. Fibroblast cells were derived from the circumcised skin tissue of a healthy 10-year-old child. The tissue collection was conducted following ethical approval and informed consent procedures in accordance with Universitas YARSI's research ethics committee guidelines (No: 277/KEP-UY/EA.10/X/2023). The cells were cultured and subcultured up to passage 3 to represent young cells and passage 24 to represent senescent cells. The cells (5000 cells/well) were treated with basic expansion medium (DMEM) and secretome medium. Medium samples were collected on days 1, 3, 5, and 7.

2.2. Isolation and Expansion of Human Dermal Fibroblast Cells

The tissue sample was transported aseptically and processed within 1 hour after collection. The skin was

washed thoroughly in sterile phosphate-buffered saline (PBS) containing 1% antibiotic-antimycotic solution (Thermo Fisher Scientific, Waltham, MA, USA) to reduce microbial contamination. Subcutaneous fat was carefully removed using sterile scalpels. The skin was then cut into small pieces measuring approximately 1–2 mm². These explants were placed dermis-side down in T25 culture flasks pre-coated with a minimal volume of Dulbecco's Modified Eagle Medium (DMEM) supplemented with 10% Fetal Bovine Serum (FBS) and 1% antibiotic-antimycotic (Thermo Fisher Scientific, Waltham, MA, USA) to facilitate attachment. After allowing the explants to adhere for 30 minutes at room temperature, additional growth medium (DMEM with 10% FBS and 1% antibiotic-antimycotic) was gently added to cover the explants. Cultures were incubated at 37°C in a humidified atmosphere containing 5% CO₂. Medium was changed every 2–3 days, carefully avoiding disturbance of the explants. Fibroblast outgrowth from the explants was typically observed within 7–10 days. Once cells reached approximately 80% confluency, they were detached using 0.25% trypsin-EDTA (Thermo Fisher Scientific, Waltham, MA, USA) and passaged for further expansion. Cells were cryopreserved in fetal bovine serum supplemented with 10% dimethyl sulfoxide (DMSO) following standard protocols.

2.3. Fibroblast Subculture Results for Senescent Cell Determination by Cumulative Population Doubling (CPD)

Senescence in fibroblast cells was induced by replicative exhaustion, following the well-established "Hayflick limit" principle, which states that normal human fibroblasts undergo approximately 40 to 60 population doublings before permanently exiting the cell cycle. To accurately determine senescence, we used cumulative population doubling (CPD) rather than passage number alone, as CPD better reflects cells' actual replicative history. Human fibroblasts cultured under standard conditions typically enter senescence around CPD 50, characterized by irreversible growth arrest, increased senescence-associated β -galactosidase (SA- β -gal) activity, and markedly reduced DNA synthesis. Other studies have shown that the doubling time (DT) is 202 hours for fibroblast cell samples derived from a 60-year-old menopausal woman who has been menopausal for 5 years. In this study, fibroblasts were subcultured continuously for six months, and CPD was calculated using the formula: [10-13].

$$[\text{Log}_{10}(\text{harvested cell number} / \text{seeded cell number}) / \text{Log}_{10}(2)]$$

Based on the subculture data, cells at passage 24 (P24) exceeded CPD 50 and exhibited a doubling time greater than 202 hours, consistent with senescent phenotypes reported in previous studies. The reduction in CPD increments observed at later passages (P20–P25) indicates the onset of cellular aging or replicative senescence, a common feature in primary cell cultures. This study relied on CPD and growth kinetics as robust and quantitative indicators of replicative senescence (Fig. 1).

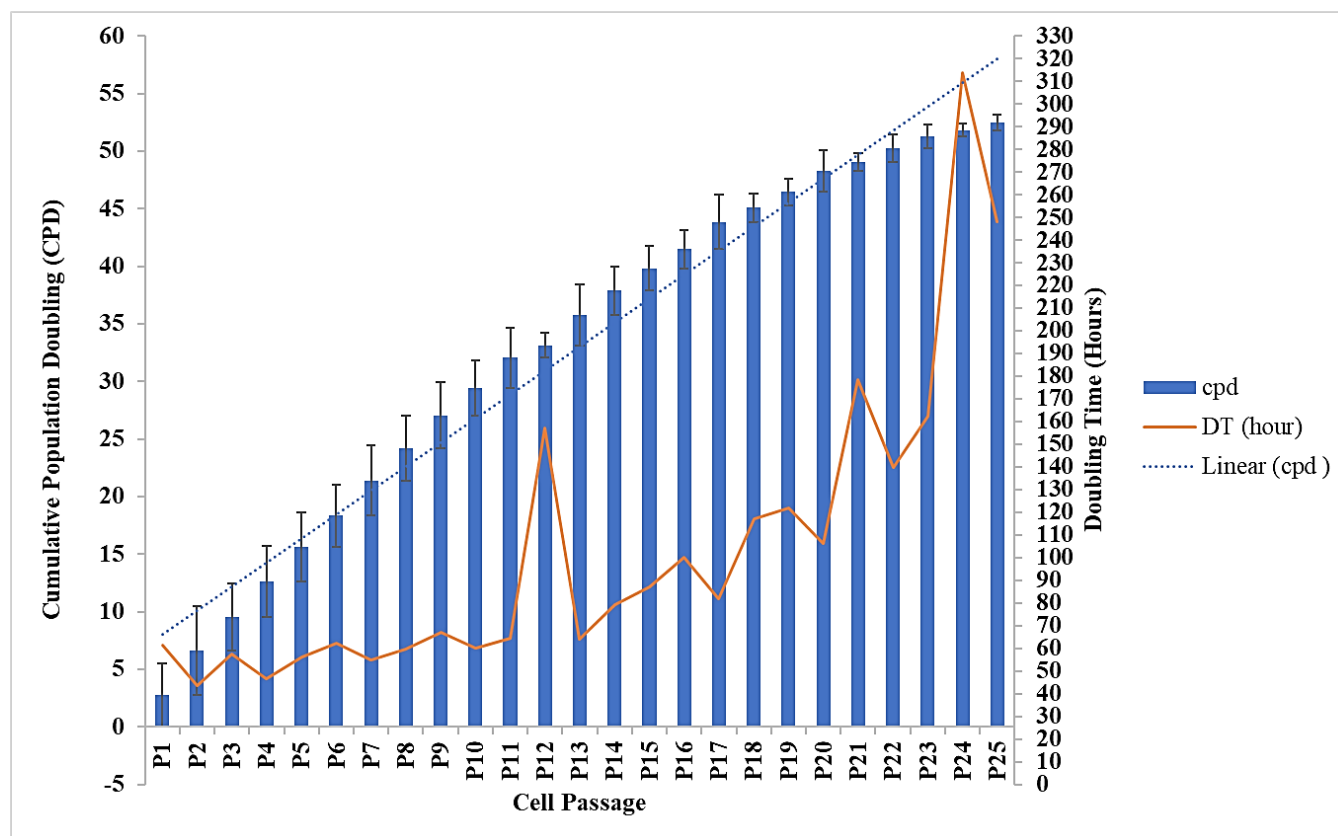


Fig. (1). Cumulative population doubling (CPD) and doubling time (DT) of subcultured fibroblast cells. Data represent mean \pm SD from $n = 3$ replications, with 250,000 cells seeded per passage. Results are presented descriptively to identify passages of cumulative population doubling (CPD) exceeding 50 and doubling time (DT) exceeding 202 hours.

2.4. Fibroblast Secretome Preparation

Human dermal fibroblast cells (5,000,000 cells/well) on Passage 5 were cultured in 870 cm² cell culture flasks using Dulbecco's Modified Eagle Medium (DMEM) supplemented with Knockout Serum Replacement (KOSR) and Antibiotic-Antimycotic until reaching 80–90% confluency (Thermo Fisher Scientific, Waltham, MA, USA). KOSR was used as an animal-free serum alternative to minimize the presence of animal-derived proteins. The cells were cultured for 1 week before secretome collection. To prepare for secretome collection, the cells were washed three times with sterile phosphate-buffered saline (PBS) to remove residual serum proteins, then incubated in 200 mL of serum-free DMEM containing KOSR and Antibiotic-Antimycotic for 24 hours at 37°C in a humidified atmosphere with 5% CO₂. The secretome was collected once after this incubation period. The conditioned medium was collected and centrifuged at 400 \times g for 8 minutes at 4°C twice to remove cellular debris and dead cells. The supernatant was then filtered through a sterile 0.22 μ m syringe filter to ensure removal of any remaining particulates. The filtered secretome was aliquoted into smaller volumes to avoid repeated freeze-thaw cycles and stored at -80°C until further use.

Following medium collection, all fibroblast cells were harvested, counted, and cryopreserved for future use. The 10% secretome medium was prepared by mixing 10% (v/v) secretome with 90% (v/v) DMEM, while the 20% secretome medium was prepared by combining 20% (v/v) secretome with 80% (v/v) DMEM [14].

2.5. Fibroblast Cell Proliferation Examination Procedure

The fibroblast cell proliferation examination procedure was performed by first discarding the medium from each well and rinsing with PBS to remove residual medium. Subsequently, 10 μ L of Cell Counting Kit-8 (CCK-8) reagent (Dojindo Laboratories, Kumamoto, Japan) was added to each well, along with 100 μ L of Dulbecco's Modified Eagle Medium (DMEM), and the mixture was incubated for 60 minutes at 37°C in a humidified atmosphere with 5% CO₂. After incubation, the absorbance was measured at 450 nm using a microplate reader.

2.6. Total Protein Examination Procedure

Total protein concentration was determined using the Coomassie (Bradford) protein assay kit (Thermo Fisher Scientific, Waltham, MA, USA) according to the manufacturer's instructions. Briefly, 5 μ L of each protein

standard and sample were pipetted into individual wells of a 96-well microplate. Afterward, 250 μL of Coomassie Brilliant Blue reagent was added to each well, and the plate was incubated at room temperature for 10 minutes to allow the dye to bind to the proteins.

The absorbance was measured at 595 nm using a microplate reader (specify model if available). All samples and standards were assayed in triplicate ($n=3$) to ensure accuracy and reproducibility. Protein concentrations were calculated based on a standard curve generated from known concentrations of bovine serum albumin (BSA). Data are presented as mean \pm standard deviation (SD).

2.7. Keratinocyte Growth Factor (KGF) Examination Procedure

Initially, 100 μL of standards and samples were added to each well of the ELISA plate and incubated for 90 minutes to allow binding (FineTest, Wuhan, China). After incubation, the wells were washed twice. 100 μL of biotin-labeled antibody was added to each well and incubated for 60 minutes. The wells were then washed three times, followed by the addition of 100 μL of SABC (streptavidin-biotin complex) solution to each well and incubation for 30 minutes. After this step, the wells were washed 5 times to remove excess reagents. Subsequently, 90 μL of TMB substrate was added to each well and incubated for 10–20 minutes, allowing color development. Finally, 50 μL of stop solution was added to each well, and the absorbance was immediately measured at 450 nm using a microplate reader.

2.8. Mek 1/2 Examination Procedure

MEK1/2 activation levels were quantified using a commercial ELISA kit (MyBioSource, San Diego, CA, USA) according to the manufacturer's protocol, with minor modifications. Briefly, 100 μL of standards and samples were added to each well of the ELISA plate, while 100 μL of phosphate-buffered saline (PBS) was added to blank wells. Subsequently, 10 μL of balance solution was added to each sample well. Then, 50 μL of conjugate solution was added to all standard and sample wells, excluding blanks. The plate was incubated at room temperature for 1 hour to allow antigen-antibody binding. After incubation, wells were washed five times with wash buffer to remove unbound substances. Next, 50 μL each of substrate A and substrate B was added to all wells, followed by incubation for 15–20 minutes at room temperature in the dark to develop color. The reaction was stopped by adding 50 μL of stop solution to each well. Absorbance was immediately measured at 450 nm using a microplate reader (specify model if available). All samples were assayed in triplicate ($n=3$) to ensure reproducibility. MEK1/2 activation levels were calculated based on the standard curve generated from known concentrations. Data were expressed as mean \pm standard deviation (SD). The MEK1/2 activation was assessed by comparing treated samples with untreated control cells to determine the effect of fibroblast secretome on MEK1/2 phosphorylation. Untreated cells cultured in basic medium served as negative controls,

allowing for the evaluation of secretome-induced changes in MEK1/2 activation.

2.9. Type-1 Collagen Examination Procedure

Initially, 100 μL of standards and samples were added to each well and incubated for 2 hours to allow antigen binding (MyBioSource, San Diego, CA, USA). After incubation, the liquid in the wells was discarded without washing. Subsequently, 100 μL of reagent A was added to all wells, followed by a 1-hour incubation. The wells were then emptied and washed three times. Next, 100 μL of reagent B was added to each well and incubated for 30 minutes. After this incubation, the wells were discarded and washed five times. Then, 90 μL of substrate solution was added to all wells and incubated for 10–20 minutes to develop color. Finally, 50 μL of stop solution was added to each well, and the absorbance was immediately measured at 450 nm using a microplate reader.

2.10. Data Analysis

The data from P3 and P24 were analyzed for normality and homogeneity using the Kolmogorov-Smirnov and Levene tests, respectively. If the data met the assumptions of normal distribution and homogeneity of variance, a one-way analysis of variance (ANOVA) was conducted, followed by post hoc analysis for multiple comparisons. Statistical significance was determined at a p -value of less than 0.05.

3. RESULTS

3.1. Fibroblast Secretome at 20% Concentration Promotes Senescent Cell Proliferation

The proliferation of fibroblast cells at day 1 was $5207,11 \pm 439,04$ cells/well in P3-D10, $10797,89 \pm 805,67$ cells/well in P24-D10, $10980,22 \pm 717,88$ cells/well in P24-S10, and $11354,89 \pm 1162,5$ cells/well in P24-S20. At day 3, the proliferation of fibroblast cells was $22790,00 \pm 437,66$ cells/well in P3-D10, $15948,33 \pm 2544,7$ cells/well in P24-D10, $14050,67 \pm 2158,43$ cells/well in P24-S10, and $15028,67 \pm 1748,83$ cells/well in P24-S20. At day 5, the proliferation of fibroblast cells was $42268,67 \pm 7536,39$ cells/well in P3-D10, $14637 \pm 2250,57$ cells/well in P24-D10, $18245 \pm 2304,27$ cells/well in P24-S10, and $21135,67 \pm 1392,89$ cells/well in P24-S20. At day 7, the proliferation of fibroblast cells was $64703,34 \pm 2729,01$ cells/well in P3-D10, $21657,5 \pm 867,13$ cells/well in P24-D10, $25468,75 \pm 3249,12$ cells/well in P24-S10, and $30342,5 \pm 910,41$ cells/well in P24-S20 (Fig. 2).

The analysis revealed a significant increase in cell proliferation in treatment group 2 (P24-S20) compared to the negative control (P24-D10) on both day 5 and day 7, indicating that higher concentrations of secretome medium can enhance cell proliferation in senescent cells. Senescent cells treated with 20% secretome showed a significant 44% increase in proliferation on day 5 ($21135,67 \pm 1392,89$ cells/well) compared to untreated controls ($14637 \pm 2250,57$ cells/well, $p < 0.05$). Statistical analysis was performed using one-way ANOVA followed by a post hoc test, confirming that the differences between

groups were statistically significant. These results suggest a dose-dependent effect of the secretome medium on promoting cell proliferation in senescent cells (**Supplementary Material**).

On Day 1, the cell count in P3 was lower than in P24. This was caused by poor adaptation of P3 cells, which were freshly thawed and immediately cultured in well plates. In contrast, P24 cells had already adapted because they had been maintained in flasks for 3-4 weeks for cell expansion. Proliferation in the P24-S20 group was slightly higher compared to P24-D10 and P24-S10, indicating that

the 20% secretome medium was more effective than the DMEM medium or 10% secretome medium in promoting senescent cell proliferation (Fig. 3).

Day 3, proliferation in P3 had surpassed that of all P24 groups, indicating that P3 cells had adapted well to the environment and exhibited a higher exponential growth rate than all other groups. At this phase, the DMEM medium in the P24 group showed the highest effectiveness, followed by the 20% secretome medium, and the 10% secretome medium had the lowest effectiveness (Fig. 4).

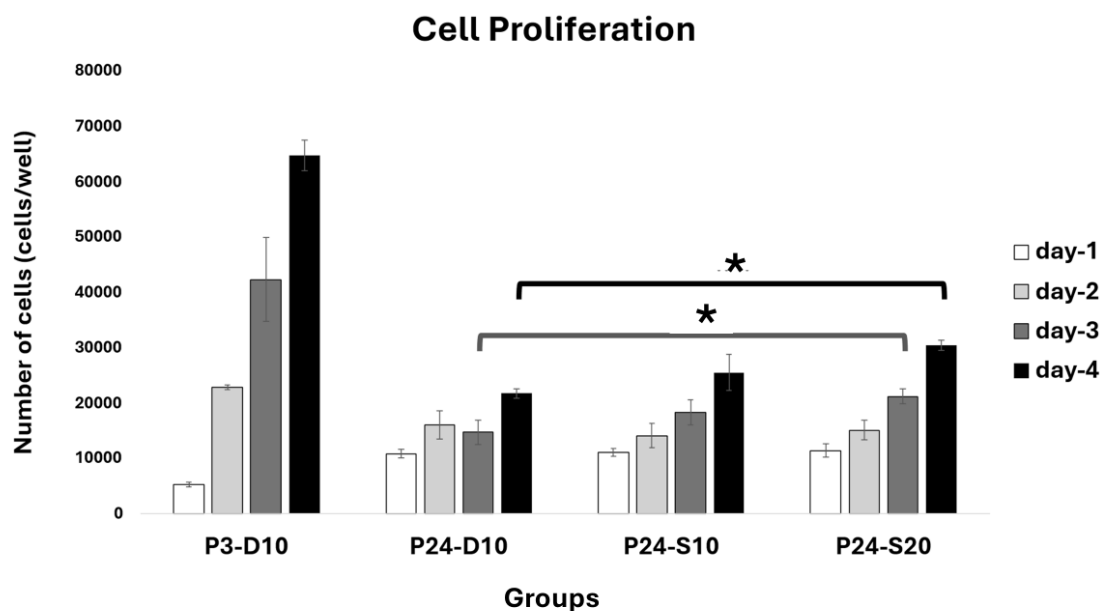
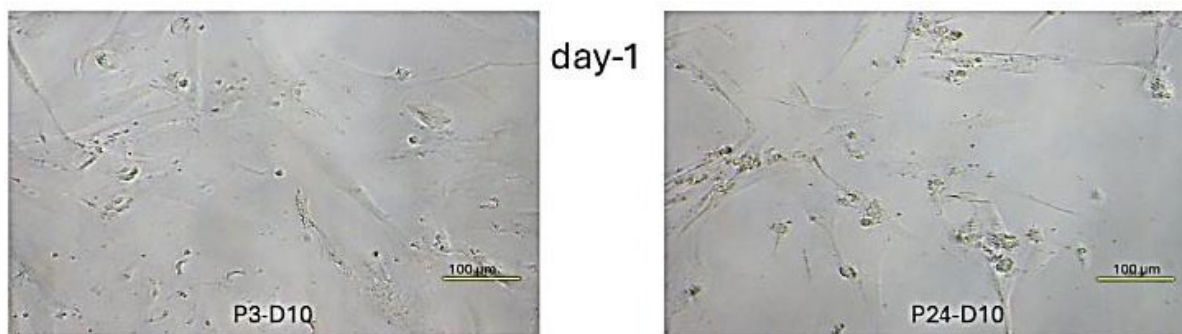


Fig. (2). Cell proliferation profile after treatment. Data represent mean \pm SD from $n = 3$ replications, with 5,000 cells seeded per well. P3-D10: Passage 3 fibroblasts in DMEM+FBS10%, P24-D10: Passage 24 fibroblasts in DMEM+FBS10%, P24-S10: Passage 24 fibroblasts in secretome 10% and P24-S20: Passage 24 fibroblasts in secretome 20%. Cell proliferation in the P24-S20 group was higher than in the P24-D10 group on days 5 and 7. Statistical analysis was performed using one-way ANOVA followed by post hoc test ($*p < 0,05$).



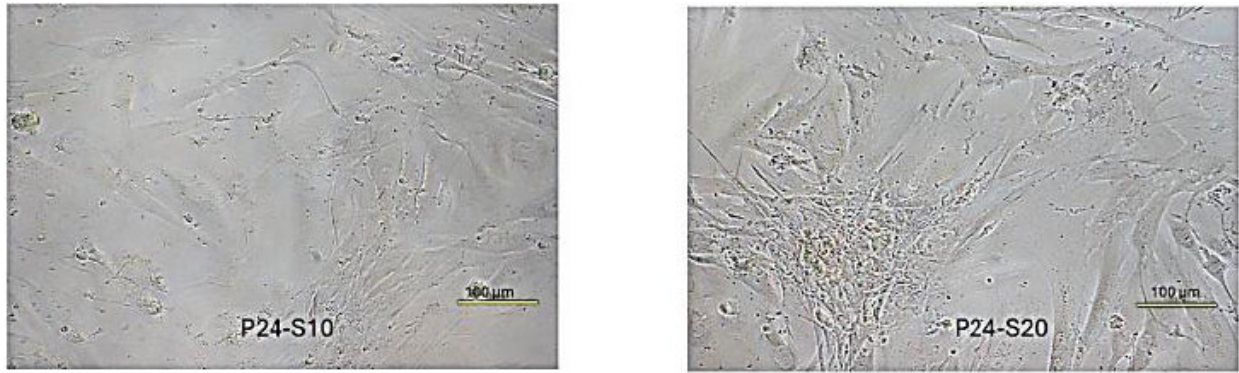


Fig. (3). Fibroblast cell confluence day-1. **P3-D10.** Relatively sparse fibroblast cell growth confluence, with characteristic spindle-shaped morphology. **P24-D10.** Much higher cell density with more fibroblasts visible per field. Cells appear more densely packed. **P24-S10.** Slightly more densely packed compared to the negative control group. **P24-S20.** The highest cell density among all groups. The cell layer is nearly confluent, with some overlapping cells.

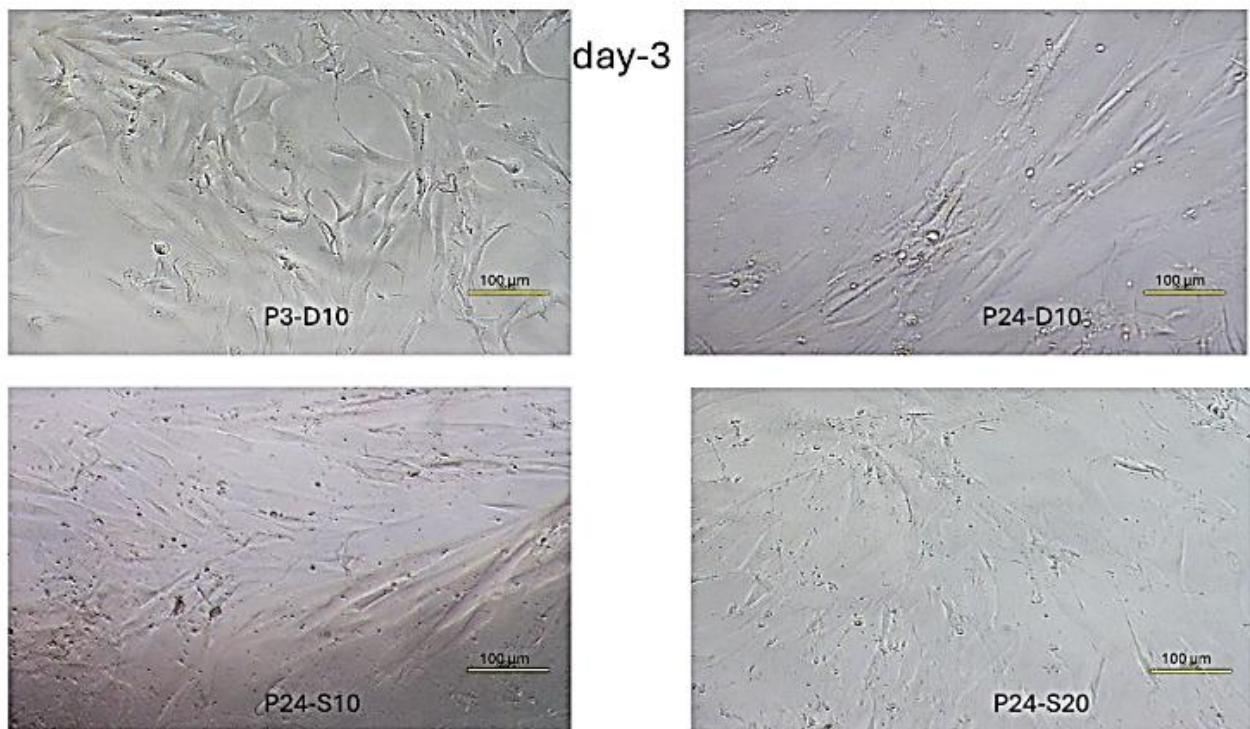


Fig. (4). Fibroblast cell confluence day-3. **P3-D10.** The highest cell density among all groups, with an almost fully confluent layer. **P24-D10.** Moderate cell density, with gaps still present between cells and a lower density compared to the young cells group. **P24-S10.** The lowest density among all groups. Some areas show dense growth, while other areas are more sparse. **P24-S20.** Slightly lower density than the negative control group. The distribution pattern is more uniform than P24-S10, with moderate confluence.

On Day 5, the P3 group showed the highest proliferation among all groups. Within the P24 groups, the highest proliferation was observed in the 20% secretome medium, followed by the 10% secretome medium, with DMEM showing the lowest effectiveness. This suggests a dose-dependent effect of the secretome medium in enhancing cell proliferation (Fig. 5).

On Day 7, the P3 group demonstrated proliferation approximately 2-3 times higher than that of all P24 groups. The increasing trend observed on day 5 continued through day 7. The response of senescent cells to the secretome medium became more evident, with the 20% secretome medium showing the highest proliferation compared to DMEM and 10% secretome media (Fig. 6).

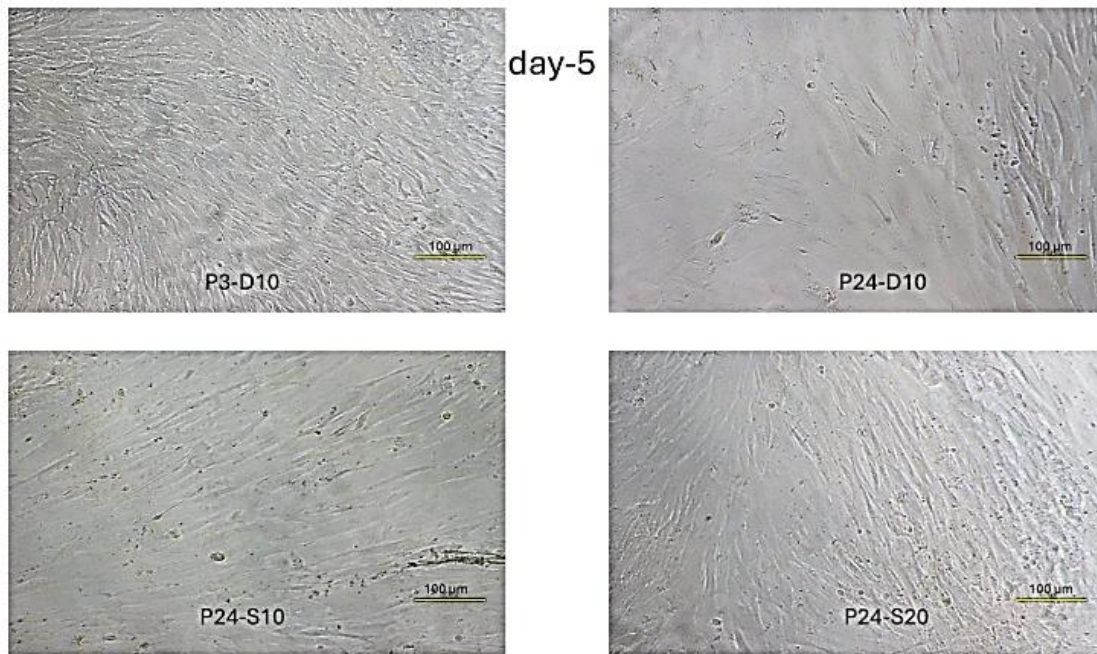


Fig. (5). Fibroblast cell confluence day-5. **P3-D10.** Shows very dense cell growth, with cells beginning to pile up on top of each other due to limited surface area. Cells are tightly packed and exhibit a swirling pattern. **P24-D10.** Growth is lower compared to day 3, indicating signs of cell detachment or death. **P24-S10.** Moderate density with slightly better growth than the negative control group. **P24-S20.** Relatively high density with proliferation spread across various areas.

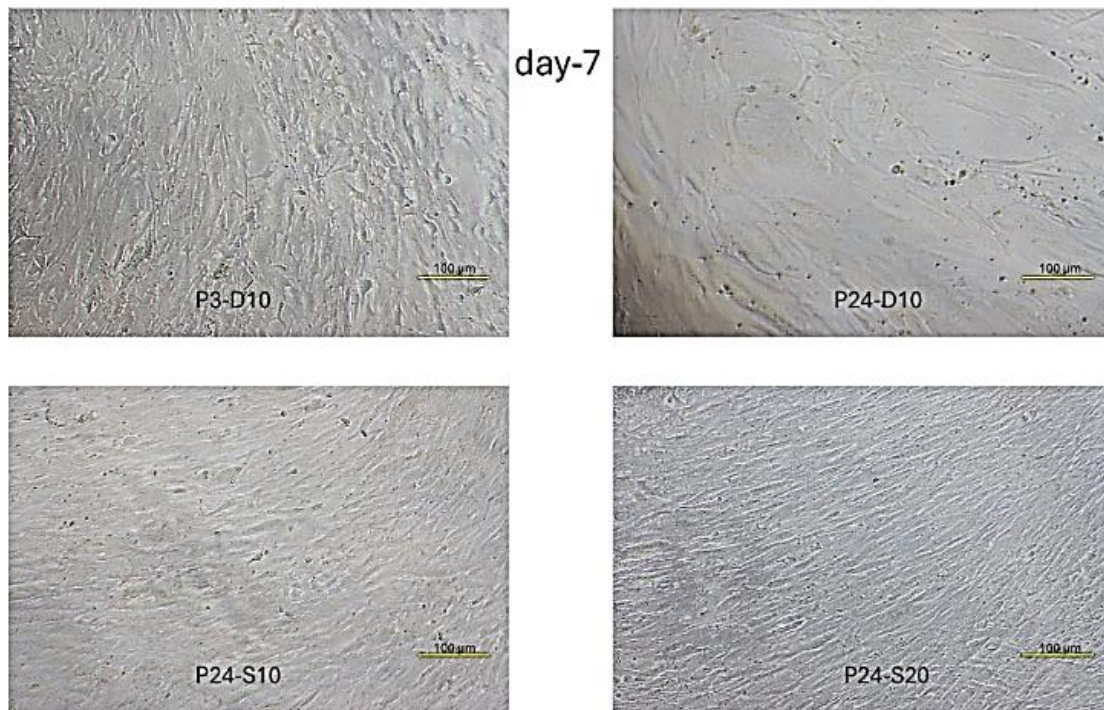


Fig. (6). Fibroblast cell confluence day-7. **P3-D10.** Very dense culture with multiple layers of cells throughout. Many cells appear compressed and show altered morphology due to extreme density caused by limited space. **P24-D10.** Single, fairly dense cell layer with near-complete confluence. **P24-S10.** Higher density than the negative control group, with nearly full confluence. **P24-S20.** The highest density level among all senescent cell groups.

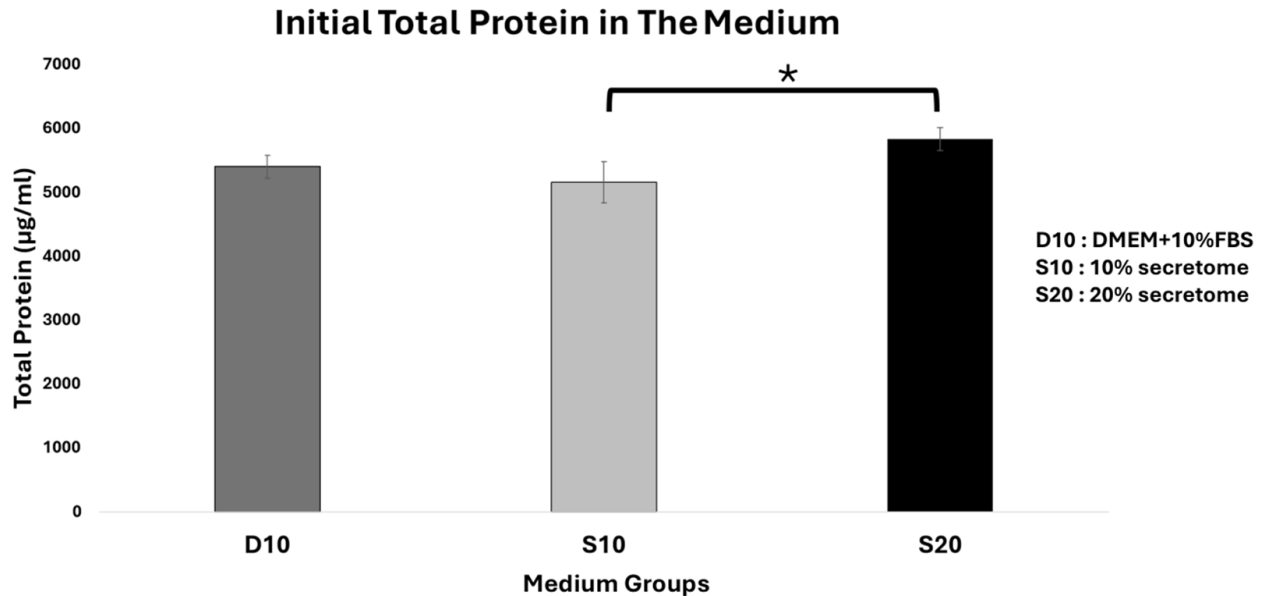


Fig. (7). Initial total protein concentration in different medium groups. Data represent mean \pm SD from $n = 3$ replications. D10: DMEM + 10% FBS, S10: 10% secretome and S20: 20% secretome. The total protein content in the 20% secretome initial medium is higher compared to the 10% secretome medium. Statistical analysis was performed using one-way ANOVA followed by post hoc test ($*p < 0,05$).

3.2. The Role of Total Proteins in the 20% Fibroblast Secretome in Enhancing Senescent Cell Proliferation

The total protein concentrations in the initial medium were $5399,33 \pm 180,69 \mu\text{g/mL}$ in D10, $5154,33 \pm 321,45 \mu\text{g/mL}$ in S10, and $5830,67 \pm 181,62 \mu\text{g/mL}$ in S20 (Fig. 7). It was found that the initial total protein amount in 20% secretome medium was the highest compared to all groups, but was significantly different only from the 10% secretome medium ($p < 0,05$).

The initial total protein amount reflects the total protein content of the starting medium before it is distributed to each group. The initial total protein in the 20% secretome medium is the highest among all groups, indicating that this medium contains more bioactive molecules such as growth factors (KGF, VEGF, TGF), cytokines, chemokines, extracellular matrix proteins, and amino acids needed for cell proliferation, distribution, and differentiation [15, 16]. Cell proliferation in the P24-S20 group is higher than in the other senescent cell groups.

3.3. Total Proteins Production After Treatment

On day 5, total protein productions after treatment in 10^4 cells/24 hours were $161,96 \pm 11,29 \mu\text{g/mL}$ in P3-D10, $0 \pm 10,39 \mu\text{g/mL}$ in P24-D10, $546,63 \pm 13,56 \mu\text{g/mL}$ in P24-S10, and $310,34 \pm 24,92 \mu\text{g/mL}$ in P24-S20. At day 7, the levels were $49,20 \pm 14,32 \mu\text{g/mL}$ in P3-D10, $0 \pm 5,39$

$\mu\text{g/mL}$ in P24-D10, $316,20 \pm 0,83 \mu\text{g/mL}$ in P24-S10, and $254,57 \pm 5,01 \mu\text{g/mL}$ in P24-S20 (Fig. 8).

A significant difference was found, with the total protein content in treatment group P24-S20 being notably higher than that of the negative control group (P24-D10) on both day 5 and day 7 ($p < 0,05$).

On day 5, the total protein production of 10,000 cells over 24 hours showed that the P3-D10 group produced protein at a moderate level. In the P24-D10 group, protein production could not be detected. The P24-S10 group had the highest protein production among all groups, followed by the P24-S20 group. This suggests that senescent cells given only standard medium could not be detected, likely due to cellular aging and reduced cell function, resulting in an inability to produce proteins needed by neighboring cells. In contrast, senescent cells treated with the secretome showed higher protein production than those given only the standard medium. These results indicate that the secretome can enhance cell function, increasing the ability of senescent cells to produce proteins essential for cell survival. However, there is a dose-dependent effect: the 10% secretome resulted in higher protein production than the 20% secretome, suggesting that senescent cells respond best to an optimal secretome dose, while higher doses may trigger negative feedback in the cellular environment.

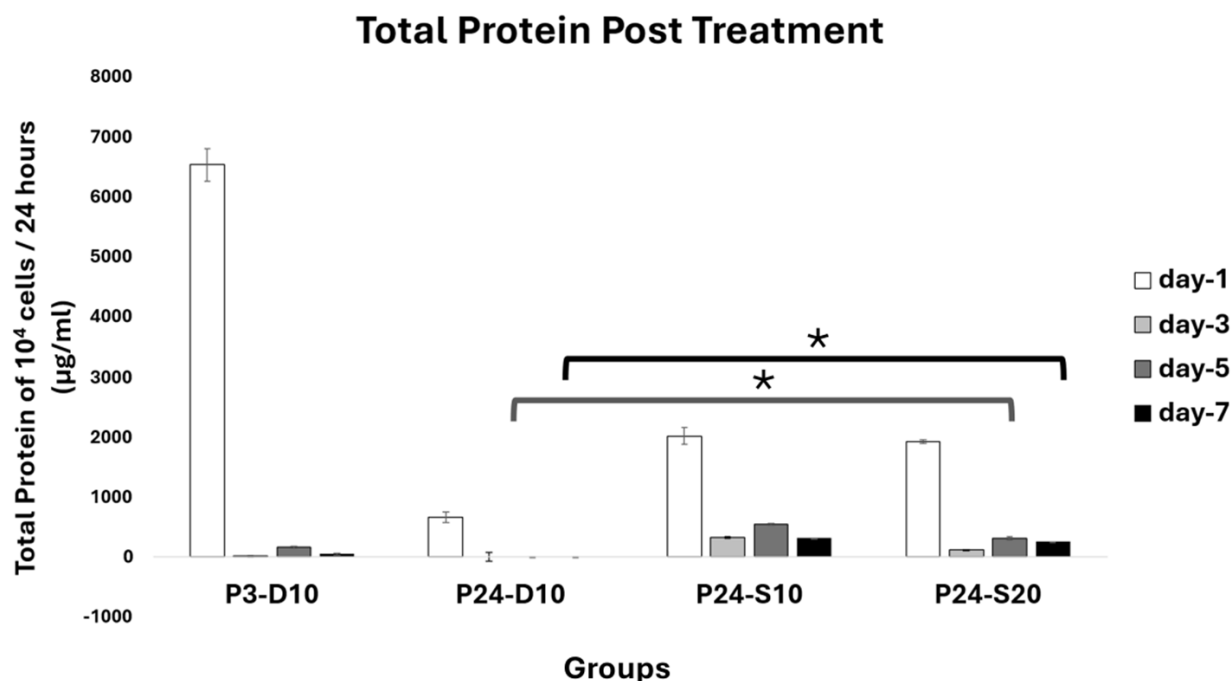


Fig. (8). Profile of total protein post treatment. Data represent mean \pm SD from $n = 3$ replications, measured from medium conditioned by 10.000 cells over 24 hours. P3-D10: Passage 3 fibroblasts in DMEM+FBS10%, P24-D10: Passage 24 fibroblasts in DMEM+FBS10%, P24-S10: Passage 24 fibroblasts in secretome 10% and P24-S20: Passage 24 fibroblasts in secretome 20%. Total protein production in P24-S20 was higher than in P3-D10 on days 5 and 7. Statistical analysis was performed using one-way ANOVA followed by post hoc test ($*p < 0,05$).

On day 7, the P3-D10 group showed decreased protein production, likely due to cells reaching high confluency, which can induce negative feedback in the cellular environment. Protein production in the P24-D10 group remained undetectable, indicating that the standard medium does not enhance protein production in senescent cells. The P24-S10 group also showed a decrease in protein production compared to day 5, and the P24-S20 group experienced a reduction as well, though less than the P24-S10 group. Overall, all groups showed a decline in protein production from day 5 to day 7, suggesting that protein utilization is maximal as cell numbers increase. These results clearly show that the secretome is effective in stimulating senescent cells to produce protein, whereas senescent cells cultured in standard medium are unable to do so.

3.4. The Role of Keratinocyte Growth Factor (KGF) in 20% Fibroblast Secretome in Enhancing Senescent Cell Proliferation

The KGF levels in the initial medium were $0,00 \pm 4,48$ pg/mL in D10, $1457,27 \pm 12,94$ pg/mL in S10, and $1712,67 \pm 7,19$ pg/mL in S20 (Fig. 9). It was found that the initial KGF level in the 20% secretome medium was higher than that in both the basic medium and the 10% secretome medium ($p < 0,05$).

The initial KGF level is the starting concentration of KGF in the medium. In the basic medium, KGF was not detected, consistent with the standard composition of DMEM and FBS, as neither is enriched in KGF. In contrast, KGF was detected in the secretome media, with the 20% secretome medium containing a higher amount of KGF than the 10% secretome medium. This is consistent with the function of skin fibroblasts, whose main protein product is KGF, a key factor in epithelial cell proliferation and tissue regeneration [4]. The KGF content in the secretome is dose-dependent; the higher the secretome concentration, the greater the KGF content.

3.5. Keratinocyte Growth Factor (KGF) Production After Treatment

At day 5, KGF levels post treatment in 10^4 cells/24 hours were 199,24 pg/mL in P3-D10, 488,95 pg/mL in P24-D10, 123,18 pg/mL in P24-S10, and 45,29 pg/mL in P24-S20. At day 7, the levels were 127,57 pg/mL in P3-D10, 369,20 pg/mL in P24-D10, 87,96 pg/mL in P24-S10, and 53,02 pg/mL in P24-S20 as shown in Fig. (10). A significant difference was found, with the KGF level in treatment group P24-S20 being lower than that of the negative control group (P24-D10) on both day 5 and day 7 ($p < 0,05$).

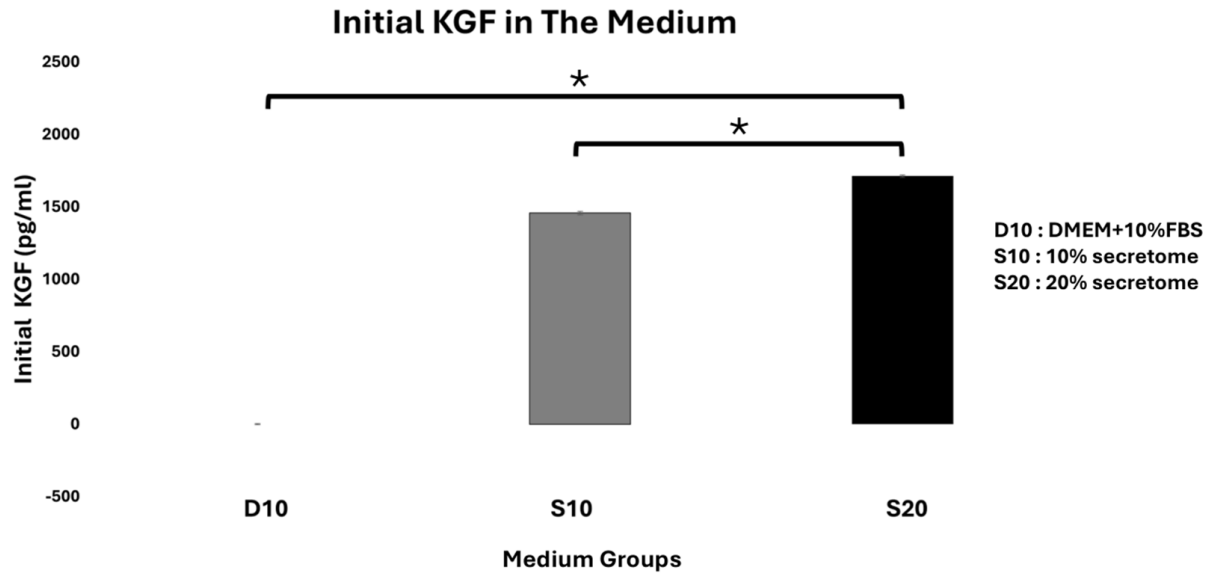


Fig. (9). Initial KGF medium profile. Data represent mean ± SD from n = 3 replications. D10: DMEM + 10% FBS, S10: 10% secretome and S20: 20%. The initial KGF level in the 20% secretome medium is higher than in the 10% secretome medium. Statistical analysis was performed using one-way ANOVA followed by a post hoc test (* $p < 0,05$).

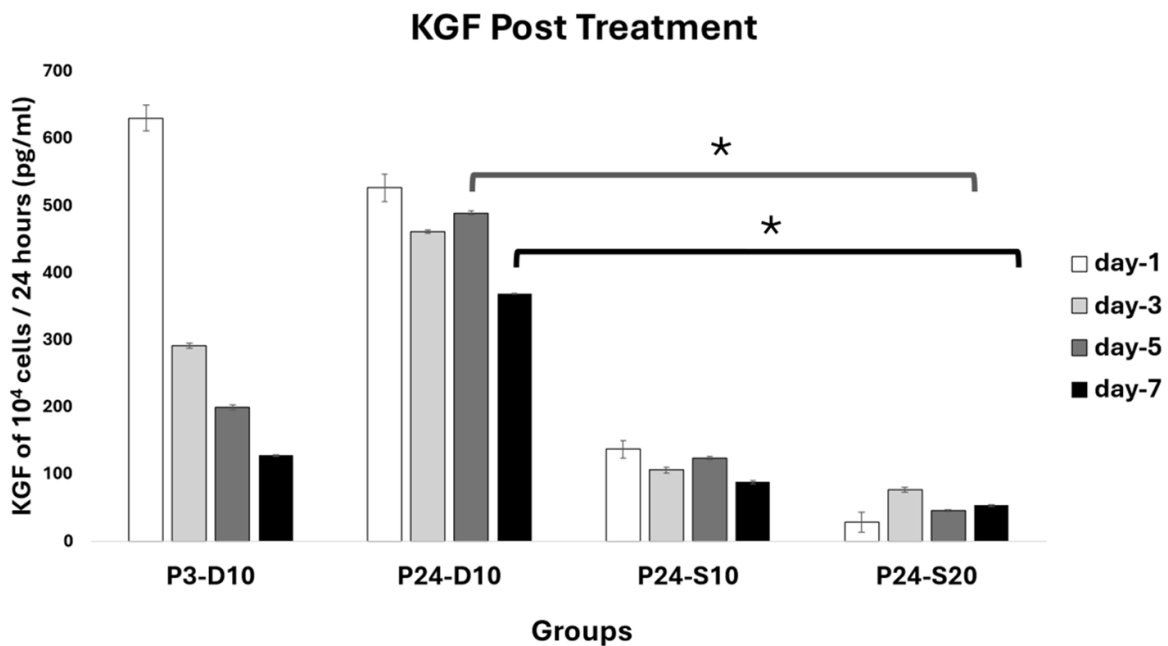


Fig. (10). KGF profile post treatment. Data represent mean ± SD from n = 3 replications, measured from medium conditioned by 10.000 cells over 24 hours. P3-D10: Passage 3 fibroblasts in DMEM+FBS10%, P24-D10: Passage 24 fibroblasts in DMEM+FBS10%, P24-S10: Passage 24 fibroblasts in secretome 10% and P24-S20: Passage 24 fibroblasts in secretome 20%. The KGF level in P24-S20 was lower than in P3-D10 on days 5 and 7. Statistical analysis was performed using one-way ANOVA followed by post hoc test (* $p < 0,05$).

On day 5 and day 7, KGF production of 10,000 cells over 24 hours showed that the P3-D10 group produced KGF at a moderate level. The P24-D10 group produced the highest KGF among all groups, which contrasts with previous findings, in which total protein production was undetectable in this group. The P24-S10 group produced a small amount of KGF, while the P24-S20 group had the lowest KGF production.

The high KGF production in the P3-D10 group suggests a compensatory mechanism: since the standard medium does not contain KGF, fibroblasts in this group produce KGF to support their own survival in a less supportive environment. In senescent cell groups treated with secretome, KGF production was lower, indicating a feedback mechanism, since the secretome medium already contains KGF, the cells produce less of it. The higher the KGF content in the secretome medium, the lower the cellular KGF production observed [17].

3.6. The 20% Fibroblast Secretome Promotes Senescent Cell Proliferation by Activating the MEK1/2 Signaling Pathway

At day 5, pMEK 1/2 levels post treatment in 10^4 cells were $0,00 \pm 0,00$ pg/mL in P3-D10, $0,01 \pm 0,00$ pg/mL in P24-D10, $0,01 \pm 0,00$ pg/mL in P24-S10, and $0,01 \pm 0,00$ pg/mL in P24-S20 at 45 minutes; while at 24 hours, the

levels were $0,08 \pm 0,00$ pg/mL in P3-D10, $0,22 \pm 0,03$ pg/mL in P24-D10, $0,22 \pm 0,02$ pg/mL in P24-S10, and $0,18 \pm 0,03$ pg/mL in P24-S20. At day 7, pMEK 1/2 levels post treatment in 10^4 cells were $0,00 \pm 0,00$ pg/mL in P3-D10, $0,01 \pm 0,00$ pg/mL in P24-D10, $0,01 \pm 0,00$ pg/mL in P24-S10, and $0,01 \pm 0,00$ pg/mL in P24-S20 at 45 minutes; while at 24 hours, the levels were $0,06 \pm 0,00$ pg/mL in P3-D10, $0,15 \pm 0,00$ pg/mL in P24-D10, $0,14 \pm 0,01$ pg/mL in P24-S10, and $0,11 \pm 0,00$ pg/mL in P24-S20 (as shown in Fig. (11)). A significant difference was found, with the pMEK 1/2 level in the P24-S20 treatment group being higher at 24 hours compared to 45 minutes post-exposure on day 5 and day 7 ($p < 0,05$).

After 45 minutes and 24 hours of medium exposure on days 5 and 7, all groups showed increased accumulation of pMEK1/2 after 24 hours of medium exposure compared to 45 minutes. MEK 1/2 activity was higher in senescent cells than in young cells. Hyperactivation of the MAPK pathway is commonly observed in senescent cells as an adaptive response to enhance proliferative capacity under suboptimal conditions [18, 19]. The lower MEK 1/2 activity in the P24-S20 group compared to the P24-S10 group suggests that the 20% secretome can more effectively modulate cellular signaling, similar to young cells, which require less MEK 1/2 activity yet still achieve high proliferation.

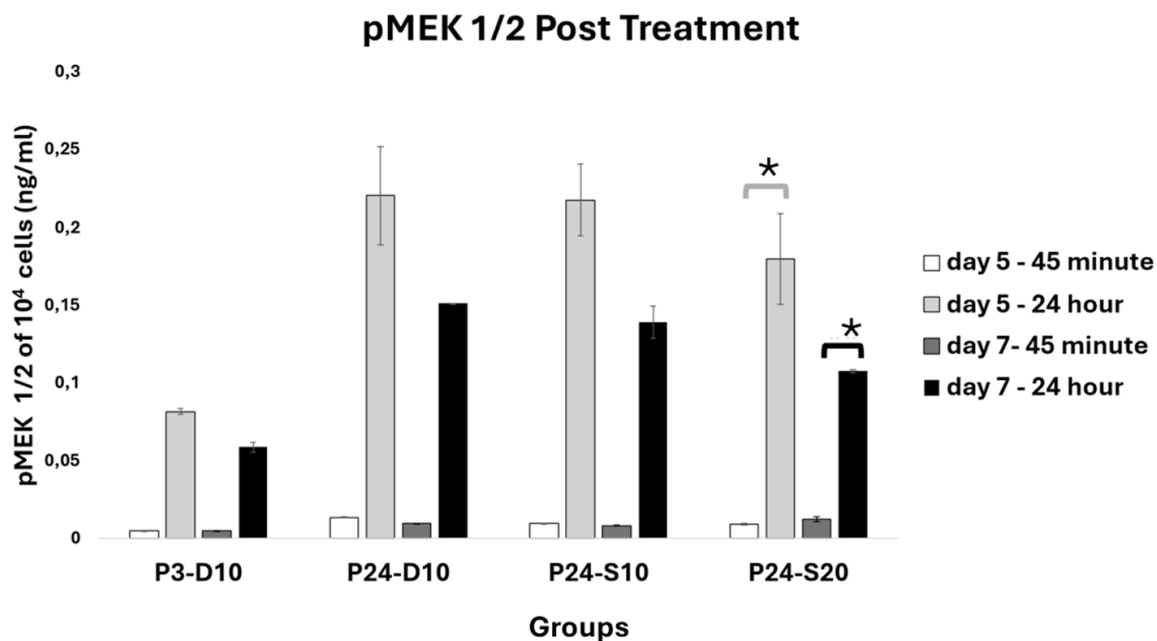


Fig. (11). pMEK 1/2 profile post treatment. Data represent mean \pm SD from $n = 3$ replications, measured from medium conditioned by 10.000 cells over 24 hours. **P3-D10:** Passage 3 fibroblasts in DMEM+FBS10%, **P24-D10:** Passage 24 fibroblasts in DMEM+FBS10%, **P24-S10:** Passage 24 fibroblasts in secretome 10% and **P24-S20:** Passage 24 fibroblasts in secretome 20%. The pMEK 1/2 level in the **P24-S20** group at 24 hours after exposure was higher than at 45 minutes after exposure. Statistical analysis was performed using one-way ANOVA followed by a post hoc test ($*p < 0,05$).

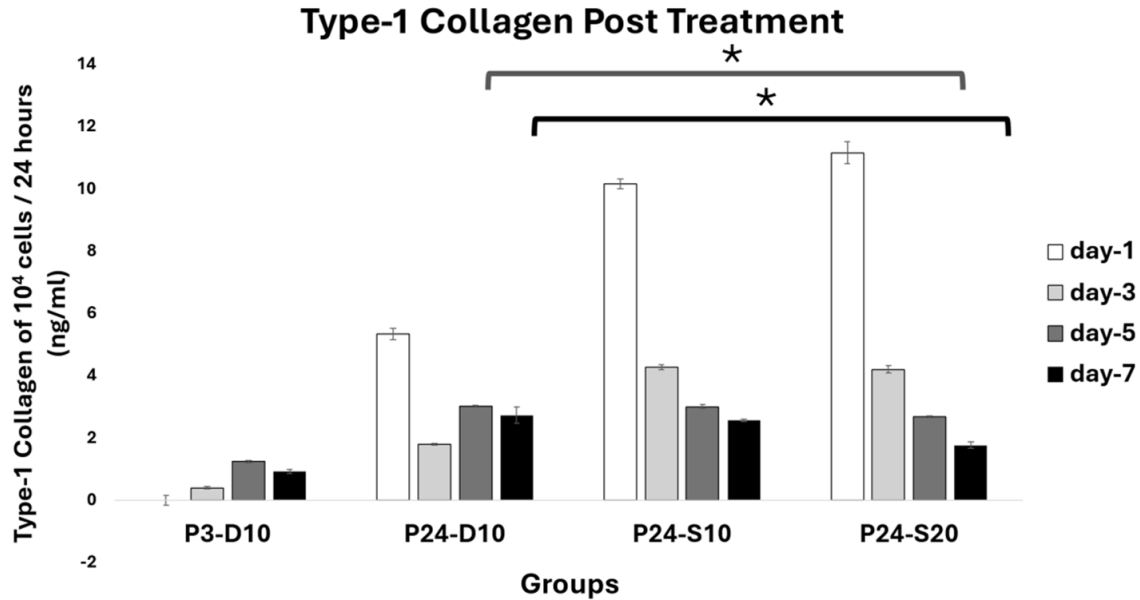


Fig. (12). Type-1 collagen profile post treatment. Data represent mean \pm SD from $n = 3$ replications, measured from medium conditioned by 10,000 cells over 24 hours. P3-D10: Passage 3 fibroblasts in DMEM+FBS10%, **P24-D10**: Passage 24 fibroblasts in DMEM+FBS10%, **P24-S10**: Passage 24 fibroblasts in secretome 10% and **P24-S20**: Passage 24 fibroblasts in secretome 20%. The type-1 collagen level of **P24-S20** was lower than that of **P24-D10** on both day 5 and day 7. Statistical analysis was performed using one-way ANOVA followed by post hoc test (* $p < 0,05$).

3.7. The 20% Fibroblast Secretome Promotes Senescent Cells Proliferation by Enhancing Type-1 Collagen Utilization

At day 5, type-1 collagen levels post treatment in 10^4 cells/24 hours were $1,23 \pm 0,04$ ng/mL in P3-D10, $3,02 \pm 0,03$ ng/mL in P24-D10, $3,00 \pm 0,06$ ng/mL in P24-S10, and $2,67 \pm 0,03$ ng/mL in P24-S20. At day 7, the levels were $0,91 \pm 0,06$ ng/mL in P3-D10, $2,73 \pm 0,26$ ng/mL in P24-D10, $2,56 \pm 0,05$ ng/mL in P24-S10, and $1,76 \pm 0,11$ ng/mL in P24-S20 as shown in Fig. (12). A significant difference was found, with the type-1 collagen level in the treatment group P24-S20 being lower than that in the negative control group (P24-D10) on days 5 and 7 ($p < 0,05$).

On days 5 and 7, type-1 collagen production by 10,000 cells over 24 hours showed that the P24-D10 group had higher type-1 collagen levels than both young cells and other senescent cell groups. In contrast, the P24-S20 group had the lowest collagen levels among all groups. Young cells exhibited high proliferation rates but low collagen production, whereas senescent cells, despite their limited proliferative capacity, could produce higher amounts of collagen [20]. The lower collagen levels in both young cells and senescent cells that were treated with 20% secretome medium suggest that type-1 collagen is being effectively utilized as an extracellular matrix to enhance cell attachment to the culture dish.

4. DISCUSSION

The proliferation pattern of Passage 3 (P3) cells showed consistent exponential growth, outperforming Passage 24 (P24) cells throughout the study. This indicates that repeated passaging reduces fibroblast proliferation potential and regenerative capacity. The growth medium plays a crucial role in enhancing senescent cell proliferation. Adding secretome to the basal medium increased proliferation rates in senescent cells compared to standard medium. Moreover, this effect was dose-dependent: cells treated with 20% secretome showed higher proliferation than those treated with 10%. The 20% secretome group exhibited a 40% increase in cell growth on day 5, which continued through day 7, compared to cells in standard medium.

The secretome is a collection of proteins, including transmembrane proteins and those secreted by cells into the extracellular space. About 13-20% of human proteins are types of secreted proteins. These cell-secreted proteins play an important role in cell migration, proliferation, signaling, and communication. Examples of cell proteins secreted by cells are enzymes, cytokines, chemokines, interferons, growth factors, colony-stimulating factors (CSFs), and tumor necrosis factors (TNFs). Secretome has an important role in regulating communication between cells, tissues, and organs; therefore, if there is a disruption, homeostasis will not run well, resulting in tissue pathophysiology and disease. Secretome can act in autocrine, paracrine, and endocrine

modes, exerting agonistic or antagonistic effects that stimulate or inhibit cellular physiological processes. Recent studies have highlighted the emerging role of the secretome in tissue regeneration and cellular senescence. Furthermore, advances in proteomic analyses have identified novel secreted factors involved in modulating senescent cell behavior and the senescence-associated secretory phenotype (SASP). Understanding the molecular components and mechanisms of secretome action not only offers insights into cell-cell communication but also opens avenues for developing secretome-based therapies for age-related diseases and tissue dysfunction [21].

A study demonstrated that secretome derived from adipose cells promotes regeneration by enhancing cell proliferation, differentiation, and migration. It also reduces the accumulation of senescent cells by lowering β -galactosidase activity and inflammatory factors [22]. Accumulation of senescent cells is a hallmark of degenerative diseases, making their removal or modulation a key therapeutic target. Senotherapeutics are divided into two categories: senolytics, which eliminate senescent cells, and senomorphics, which mitigate the harmful effects of the senescence-associated secretory phenotype (SASP). Senomorphics act by clearing SASP molecules from the cellular environment or by modifying cellular functions to maintain viability and proliferation [23].

A typical cell contains approximately 2-4 million protein molecules and can synthesize 10,000-20,000 proteins per second, resulting in an average protein production of 0.5-2 ng per cell per day. In this study, senescent cells treated with secretome produced more total protein than those in basal medium, indicating that secretome enhances their protein synthesis capacity. Notably, on days 5 and 7, protein production in secretome-treated senescent cells exceeded that of young cells. Cells subjected to repeated passaging generate diverse subpopulations, exhibit faster growth, and increase protein synthesis as part of environmental adaptation. High-passage cells show elevated glycolytic activity and modulate transcription and translation to support increased protein production. However, this heightened protein synthesis in senescent cells is not indefinite, as continuous proliferation may lead to genetic instability or mRNA dysfunction [24, 25].

The biological function of cells relies more on paracrine effects than on direct replacement of damaged cells, which is the primary role of the secretome. Both *in vitro* and *in vivo* studies show that the adipose-derived secretome, rich in Epidermal Growth Factor (EGF), Keratinocyte Growth Factor (KGF), and Hepatocyte Growth Factor (HGF), enhances the proliferation and migration of skin fibroblasts, keratinocytes, and vascular endothelial cells during wound healing [26]. KGF transcription occurs in most mesenchymal and stromal cells, particularly dermal fibroblasts. It plays key roles in anti-apoptosis, cytoprotection, proliferation, and migration through signaling pathways such as Raf/MAPK/ERK, PAK4/Akt/PI3K, Src-Cortactin/Rho/Rac/Cdc42, and

PLC γ /IP3/DAG/PKC [17, 27]. During proliferation, KGF activates the Raf/MAPK/ERK cascade. KGF production varies by cell type: fibroblasts produce 3-15 ng per million cells, mesenchymal stem cells (MSCs) 1-10 ng, osteoblasts 0.1-0.8 ng, while keratinocytes do not produce KGF.

In anti-apoptotic processes, KGF activates the PI3K/Akt pathway, reducing apoptosis gene expression. Cytoprotection is mediated by KGF through the PAK4/Akt/PI3K and ERK1/2 pathways, which increase the expression of genes that mitigate free radical-induced damage [28]. In this study, KGF levels decreased over time, likely due to energy reallocation favoring proliferation over growth factor production and contact inhibition triggered by increased cell density. These mechanisms prevent excessive cell growth. Additionally, lower KGF levels may result from its consumption in anti-apoptotic and cytoprotective functions to protect cells from death and damage [29, 30].

The most classic proliferation pathway involves MEK 1/2 activation. MEK 1/2 is a protein kinase that plays a role in the RAS-RAF-MEK-ERK pathway, also known as the mitogen-activated protein kinase (MAPK) pathway. The RAS-RAF-MEK-ERK cascade pathway is a pathway for intracellular processes such as proliferation, differentiation, and cell metabolism [31, 32]. Several growth factors and polypeptides bind to transmembrane receptors to then activate the regulation of the MAPK pathway. Ligand binding to the cell membrane activates the Shc protein, which then activates the growth factor receptor-bound protein-2 (GRB2). GRB2 will interact with son of sevenless (SOS), then SOS will convert guanosine diphosphate (GDP) to guanosine triphosphate (GTP) on the RAS G protein. RAS will then activate RAF, which will phosphorylate MEK 1/2 serine. MEK 1/2 will phosphorylate threonine and tyrosine residues of ERK 1/2, so that activated ERK 1/2 will move into the nucleus to then phosphorylate and activate various transcription factors such as Sp1, E2F, Elk-1, and AP-1 to produce proteins such as Jun and Fos. This entire process is an intracellular pathway for cell mechanisms of proliferation, migration, and differentiation [33].

Senescent cells have high MAPK pathway activity; this is a characteristic of these cells. MEK activity in this study appears higher than in young cells; this illustrates the characteristics of senescent cells. However, MEK activity in the group given 20% secretome medium is lower than in other senescent cell groups. This suggests that secretome can normalize the "hyperactive stress pathway," a characteristic of these senescent cells. By normalizing this pathway, cells can perform their functions optimally [34, 35]. Normalization of the "hyperactive stress pathway" is essential for senescent cells to reduce inflammation and prevent further tissue damage. If there is a decrease in the ability to normalize the pathway, cell damage can occur and cause senescent cells to become cancer cells. It is well known that one of the hallmarks of cancer cells is increased MAPK pathway activity. In this study, MAPK pathway activity can be reduced by the secretome while still maintaining optimal proliferation [36, 37].

The MEK1/2-ERK1/2 signaling pathway, a key component of the mitogen-activated protein kinase (MAPK) cascade, plays a central role in regulating cell proliferation, differentiation, survival, and aging, as well as tissue regeneration. This pathway transduces signals from cell surface receptors to the nucleus, influencing cell cycle progression and gene expression. In fibroblasts, MEK1/2-ERK1/2 activation promotes proliferation and extracellular matrix production, which are critical for tissue repair. However, ERK1/2 signaling plays a dual role in cellular senescence, depending on the context and activation intensity; strong or sustained activation can induce senescence through mechanisms such as nuclear translocation and feedback regulation, while moderate activation supports cell proliferation [38].

This duality underscores the complex role of MEK/ERK signaling in aging and regeneration. When compared to other mitogenic growth factors like epidermal growth factor (EGF) and fibroblast growth factor (FGF), fibroblast secretome contains a complex mixture of bioactive proteins, including keratinocyte growth factor (KGF, also known as FGF), which specifically activates MEK1/2-ERK1/2 to enhance cell proliferation and migration. While EGF and FGF also activate the MEK/ERK pathway, the secretome's synergistic combination of multiple factors may amplify or fine-tune regenerative responses more effectively than individual growth factors alone. This comparison is important to discern whether regenerative effects are primarily driven by key growth factors or by the collective action of the secretome's components [39].

Collagen plays a crucial role in maintaining fibroblast cell morphology and providing mechanical support to various tissues, especially the skin. In the young dermis, interactions between fibroblasts and collagen fibrils are strong and well-organized, helping preserve the characteristic spindle shape and size of fibroblasts and contributing to the overall structural integrity and tightness of the skin. This tight binding also supports cellular functions, such as migration, proliferation, and differentiation, that are necessary for skin homeostasis and regeneration. However, in the elderly dermis layer, the amount and quality of collagen fibrils decrease significantly, leading to weakened binding between fibroblasts and the extracellular matrix. As a result, fibroblast cells shrink and change their morphology, while the dermal tissue loses its density and elasticity, contributing to visible signs of skin aging such as wrinkles, looseness, and reduced wound healing capacity.

Collagen is the most abundant protein in the extracellular matrix (ECM) and is essential in regulating crucial cellular processes, including survival, proliferation, migration, and differentiation of fibroblasts and other cell types. *In vitro* studies widely use collagen-coated culture surfaces to mimic the native ECM environment, thereby enhancing cell adhesion by providing specific binding sites for integrins and other adhesion molecules on the cell membrane. This improved adhesion facilitates faster cell spreading and signaling, leading to accelerated cell proliferation and a shorter doubling time. Moreover, the

collagen matrix offers a protective environment that reduces cellular damage caused by oxidative stress, which is a major contributor to aging and cellular senescence. Studies have shown that culturing fibroblasts on collagen matrices not only improves their viability and growth but also enhances their resistance to apoptotic stimuli, thereby supporting cell survival under stress conditions [6].

Proteomic and mechanobiological research has revealed that collagen also participates actively in signal transduction pathways that regulate fibroblast behavior. For example, the engagement of collagen with integrin receptors activates focal adhesion kinase (FAK) and downstream signaling cascades such as MAPK/ERK and PI3K/Akt pathways, promoting cytoskeletal reorganization and gene expression linked to proliferation and extracellular matrix remodeling. This dynamic interplay underscores the importance of collagen not merely as a structural scaffold but as a bioactive regulator of cell function. Accordingly, strategies focusing on restoring collagen content and organization in aged skin are being explored for anti-aging and tissue regenerative therapies [7].

The fibroblast secretome plays a crucial role in extracellular matrix (ECM) remodeling by modulating key components such as collagen, fibronectin, and matrix metalloproteinases (MMPs). The secretome contains various proteins and growth factors that not only promote ECM synthesis but also regulate ECM degradation through MMP activity, maintaining a dynamic balance essential for fibrosis and tissue regeneration. For instance, type I and III collagens secreted by fibroblasts form the structural backbone of the ECM, while MMPs degrade aged or damaged ECM proteins, facilitating efficient tissue remodeling and repair. Alterations in secretome composition, such as increased profibrotic factors or decreased MMP inhibitors, can disrupt this balance, leading to excessive ECM accumulation and fibrosis. Moreover, the fibroblast secretome influences cell adhesion and mechanotransduction *via* integrin receptor interactions, which regulate fibroblast differentiation into myofibroblasts—cells actively involved in ECM contraction and remodeling. Therefore, the fibroblast secretome acts as a key mediator in controlling ECM structure and function during wound healing and tissue regeneration [40, 41].

In this study, young cells have high proliferation but low collagen production, while senescent cells have limited proliferation rates but can produce more collagen. This behavior is called the “division of labor phenomenon,” where cells can prioritize their work depending on their needs, the need for proliferation, or production. In the senescent cell group, it is seen that these cells prioritize collagen production over proliferation. Collagen production in the senescent cell group given 20% secretome has lower levels compared to senescent cells given base medium. This shows that as proliferation increases, the need for collagen also increases to support cell attachment in the culture dish, enabling cells to carry out their proliferative function more optimally [42].

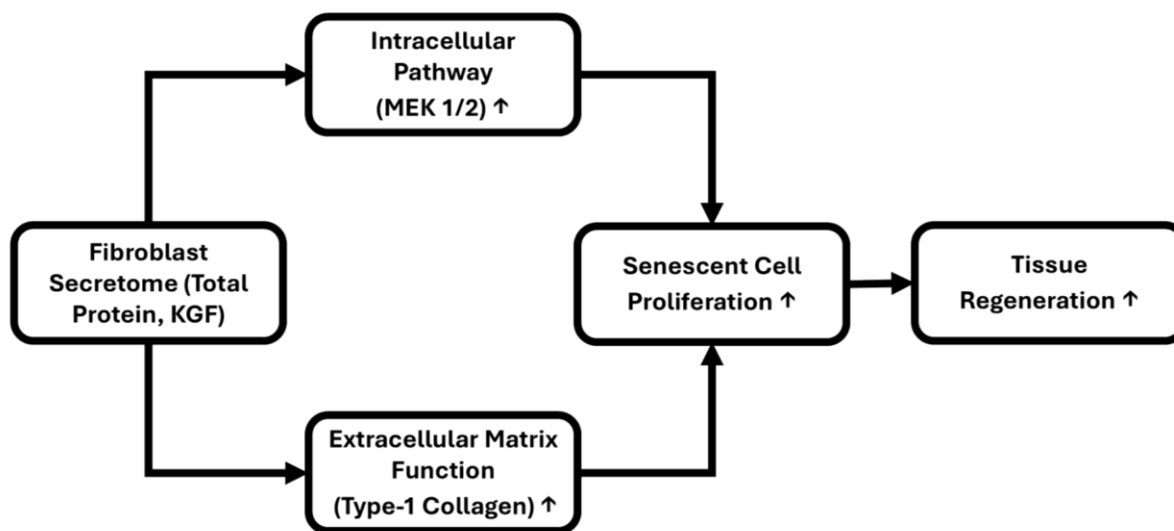


Fig. (13). Schematic representation of the proposed mechanism by which fibroblast secretome promotes tissue regeneration via intracellular and extracellular pathways.

Fibroblast secretome, characterized by total protein and keratinocyte growth factor (KGF), enhances tissue regeneration through two major mechanisms: (1) activation of the intracellular MEK 1/2 signaling pathway, leading to increased proliferation of senescent cells, and (2) improvement of extracellular matrix function, as indicated by elevated type I collagen production. Both pathways synergistically contribute to the proliferation of senescent cells and ultimately promote tissue regeneration. Arrows indicate the direction of effect (Fig. 13).

The limitations of this study are that it used an *in vitro* model with senescent cells, which have inherently limited proliferative capacity, thereby restricting analyses requiring large cell numbers. Additionally, focusing on a single signaling pathway and a limited subset of secretome components may not fully capture the complex mechanisms at play. Future research should validate these findings *in vivo* to better assess the therapeutic potential of fibroblast secretome in tissue regeneration and anti-aging. Broader proteomic profiling and investigation of multiple signaling pathways will provide a more comprehensive understanding of the secretome's biological effects. Addressing these areas will clarify the generalizability and mechanistic basis of the fibroblast secretome's impact on senescent cells.

CONCLUSION

In conclusion, this study demonstrates that treatment with 20% fibroblast secretome significantly enhances proliferation and total protein production in senescent cells *in vitro*. This effect is likely mediated by bioactive proteins in the secretome, such as keratinocyte growth factor (KGF), which are absent in the standard medium and are correlated with increased cell proliferation. The observed modulation of MEK1/2 signaling suggests that

the secretome may help regulate the hyperactive MAPK pathway associated with cellular senescence, potentially improving cell function. Increased utilization of type-1 collagen indicates enhanced extracellular matrix interactions supportive of cell attachment and growth.

These findings suggest the fibroblast secretome has potential for regenerative applications, including wound healing and anti-aging therapies. However, further *in vivo* studies are required to confirm these effects and to investigate safety, dosing, and delivery methods before clinical use. Future research should also explore optimizing secretome composition, delivery mechanisms, and long-term safety, as well as integration with biomaterial platforms and immunological evaluation.

AUTHORS' CONTRIBUTIONS

The authors confirm contribution to the paper as follows: M.R.: Designed the study, harvested the fibroblast cells, performed most of the work involving cell cultures, sample preparation for analysis, and data interpretation, and wrote the manuscript; I.K.: Designed the study, provided expert assistance with harvesting and culturing the cells, and revised the manuscript; R.S.H. and R.: Assisted with optimizing the protocol for sample preparation for analysis and revised the manuscript; E.P., H.M. and D.M.: Provided expert assistance with sample preparation for analysis and data interpretation and revised the manuscript. All authors read and approved the final manuscript.

LIST OF ABBREVIATIONS

KGF	= Keratinocyte Growth Factor
MEK 1/2	= Mitogen-Activated Protein Kinase Kinase 1/2

pMEK 1/2	= Phosphorylated MEK 1/2
DMEM	= Dulbecco's Modified Eagle Medium
CSFs	= Colony Stimulating Factors
MSCs	= Mesenchymal Stem Cells
TNFs	= Tumor Necrosis Factors
FGF-7	= Fibroblast Growth Factor 7
FGFR2-IIIb/KGFR	= Fibroblast Growth Factor Receptor 2-IIIb/Keratinocyte Growth Factor Receptor
Ras/MAPK	= Ras/Mitogen-Activated Protein Kinase
PI3K/AKT	= Phosphoinositide 3-Kinase/Protein Kinase B
ERK	= Extracellular Signal-Regulated Kinase
MAPKK	= Mitogen-Activated Protein Kinase Kinase
ECM	= Extracellular Matrix
PBS	= Phosphate Buffered Saline
EDTA	= Ethylenediaminetetraacetic Acid
DMSO	= Dimethyl Sulfoxide
v/v	= Volume per Volume
CCK-8	= Cell Counting Kit-8
CO ₂	= Carbon Dioxide
ELISA	= Enzyme-Linked Immunosorbent Assay
TMB	= 3,3',5,5'-Tetramethylbenzidine
VEGF	= Vascular Endothelial Growth Factor
TGF	= Transforming Growth Factor
SASP	= Senescence-Associated Secretory Phenotype
HGF	= Hepatocyte Growth Factor
Src-Cortactin/ Rho/Rac/Cdc42	= Signaling Pathways
GRB2	= Growth Factor Receptor-Bound Protein 2
SOS	= Son of Sevenless
GDP	= Guanosine Diphosphate
GTP	= Guanosine Triphosphate

ETHICS APPROVAL AND CONSENT TO PARTICIPATE

The experimental protocol for this study was reviewed and approved by the Research Ethics Committee of YARSI University, Indonesia (Approval No: 277/KEP-UY/EA.10/X/2023) under the project title, "The Role of the

Concentrated Fibroblast Secretome in Improving the Function of Fibroblast Senescent Cells" on October 16, 2023. All procedures involving cell cultures were conducted in accordance with the Institutional Research Committee's ethical standards.

HUMAN AND ANIMAL RIGHTS

All procedures performed in studies involving human participants were in accordance with the ethical standards of institutional and/or research committee and with the 1975 Declaration of Helsinki, as revised in 2013.

CONSENT FOR PUBLICATION

Written informed consent was obtained from the legal guardians of the participant.

AVAILABILITY OF DATA AND MATERIALS

All data and materials relevant to this study are included as supplementary files. The datasets and materials are also available from the corresponding author [M.R.] upon reasonable request.

FUNDING

This research was supported by the YARSI University Foundation, Indonesia under Grant No. 005/INT/PTB/DOS/YY/I.2023.

CONFLICT OF INTEREST

The authors declare no conflict of interest, financial or otherwise.

ACKNOWLEDGEMENTS

The authors acknowledge the Research Institute of YARSI University, the Doctoral Program in Biomedical Sciences of YARSI University, and the Medical Faculty of YARSI University for providing the research facilities and equipment essential for our experiments. They would like to express our sincere gratitude to the laboratory staff and research assistants who supported this study.

SUPPLEMENTARY MATERIAL

Supplementary material is available on the Publisher's website along with the published article.

REFERENCES

- [1] WHO decade healthy ageing. Geneva: WHO Press 2021.
- [2] Flint B, Tadi P. Physiology, aging. StatPearls. Treasure Island (FL): StatPearls Publishing 2025.
- [3] Lee H, Kim J, Park S. Proteomic analysis of human dermal fibroblast-conditioned media reveals key secretory proteins promoting wound repair. *Int J Mol Sci* 2024; 25(2): 789.
- [4] Amidzadeh Z, Yasami-Khiabani S, Rahimi H, *et al.* Enhancement of keratinocyte growth factor potential in inducing adipose-derived stem cells differentiation into keratinocytes by collagen-targeting. *J Cell Mol Med* 2022; 26(23): 5929-42. <http://dx.doi.org/10.1111/jcmm.17619> PMID: 36412036
- [5] Serra M, Lopez J, Martinez R. A fibroblast-derived secretome stimulates tumor growth and invasiveness via MAPK signaling. *Cancers* 2024; 16(14): 2498. <http://dx.doi.org/10.3390/cancers16142498> PMID: 39061138
- [6] Vierkötter A, Krutmann J. Oxidative stress and human skin

- connective tissue aging. *Int J Mol Sci* 2024; 25(3): 1288.
- [7] Chen X, Song X, Li Y. Collagen matrix enhances adhesion, survival, and proliferation of mesenchymal stem cells for tissue engineering applications. *J Biomed Mater Res A* 2023; 111(5): 1032-42.
- [8] Smith J, Lee A. MEK1/2 signaling in fibroblast activation and aging reversal. *J Cell Biol* 2023; 220(4): e20221234.
- [9] Kim H, Park S, Choi Y. Role of KGF in keratinocyte proliferation via MEK1/2 pathway. *Mol Med Rep* 2022; 25(1): 45-53.
- [10] Ogrodnik M. Cellular aging beyond cellular senescence: Markers of senescence prior to cell cycle arrest *in vitro* and *in vivo*. *Aging Cell* 2021; 20(4): e13338. <http://dx.doi.org/10.1111/ace1.13338> PMID: 33711211
- [11] Su Y. Extracellular vesicles rejuvenate p16INK4a+ senescent fibroblasts by activating Erk/Akt signaling. *Stem Cell Res Ther* 2023; 14(1): 78.
- [12] Lämmermann I, Terlecki-Zaniewicz L, Weinmüller R, *et al.* Blocking negative effects of senescence in human skin fibroblasts with a plant extract. *NPJ Aging Mech Dis* 2018; 4(1): 4. <http://dx.doi.org/10.1038/s41514-018-0023-5> PMID: 29675264
- [13] Yusharyahya SN, Bramono K, Sutanto NR, Kusuma I. The effect of *Trigonella foenum-graceum* L. (Fenugreek) towards collagen type I alpha 1 (COL1A1) and collagen type III alpha 1 (COL3A1) on postmenopausal woman's fibroblast. *Nat Prod Sci* 2019; 25(3): 208-14. <http://dx.doi.org/10.20307/nps.2019.25.3.208>
- [14] Zhou Y. Proteomic profiling of fibroblast secretome reveals key factors in tissue regeneration. *J Proteomics* 2021; 234: 104076.
- [15] Tan KY, Teo KL, Lim JFY, Chen AKL, Reuveny S, Oh SKW. Serum-free media formulations are cell line-specific and require optimization for microcarrier culture. *Stem Cell Res Ther* 2020; 11(1): 123.
- [16] Schneider M. Secretion profiles of KGF, FGFb, VEGF, HGF, and TGFβ1 in human dermal fibroblasts under hypoxic conditions. *J Cell Physiol* 2021; 236(5): 3792-803.
- [17] Russo B, Brembilla NC, Chizzolini C. Interplay between keratinocytes and fibroblasts: A systematic review providing a new angle for understanding skin fibrotic disorders. *Front Immunol* 2020; 11: 648. <http://dx.doi.org/10.3389/fimmu.2020.00648> PMID: 32477322
- [18] Anerillas C, Altés G, Gorospe M. MAPKs in the early steps of senescence implemEMTation. *Front Cell Dev Biol* 2023; 11: 1083401. <http://dx.doi.org/10.3389/fcell.2023.1083401> PMID: 37009481
- [19] Pang K, Wang W, Qin JX, *et al.* Role of protein phosphorylation in cell signaling, disease, and the intervention therapy. *MedComm* 2022; 3(4): e175. <http://dx.doi.org/10.1002/mco2.175> PMID: 36349142
- [20] Fullard N, Wordsworth J, Welsh C, *et al.* Cell senescence-independent changes of human skin fibroblasts with age. *Cells* 2024; 13(8): 659. <http://dx.doi.org/10.3390/cells13080659> PMID: 38667274
- [21] Jin Z. Advances in secretome analysis: Methodologies and applications in regenerative medicine. *Biochim Biophys Acta Proteins Proteomics* 2021; 1869(6): 140581.
- [22] Mitchell R, Mellows B, Sheard J, *et al.* Secretome of adipose-derived mesenchymal stem cells promotes skeletal muscle regeneration through synergistic action of extracellular vesicle cargo and soluble proteins. *Stem Cell Res Ther* 2019; 10(1): 116. <http://dx.doi.org/10.1186/s13287-019-1213-1> PMID: 30953537
- [23] Saoudaoui S, Bernard M, Cardin GB, Malaquin N, Christopoulos A, Rodier F. mTOR as a senescence manipulation target: A forked road. *Adv Cancer Res* 2021; 150: 335-63. <http://dx.doi.org/10.1016/bs.acr.2021.02.002> PMID: 33858600
- [24] Nöbel M, Barry C, MacDonald MA. Harnessing metabolic plasticity in CHO cells for enhanced perfusion cultivation. *Appl Microbiol Biotechnol* 2023; 107(1): 123-37.
- [25] Milo R, Phillips R. *Cell biology by the numbers*. Boca Raton, FL: CRC Press 2015. <http://dx.doi.org/10.1201/9780429258770>
- [26] Park SR, Kim JW, Jun HS, Roh JY, Lee HY, Hong IS. Stem cell secretome and its effect on cellular mechanisms relevant to wound healing. *Mol Ther* 2018; 26(2): 606-17. <http://dx.doi.org/10.1016/j.ymthe.2017.09.023> PMID: 29066165
- [27] Sadeghi S, Kalhor H, Panahi M, *et al.* Keratinocyte growth factor in focus: A comprehensive review from structural and functional aspects to therapeutic applications of palifermin. *Int J Biol Macromol* 2021; 191: 1175-90. <http://dx.doi.org/10.1016/j.ijbiomac.2021.09.151> PMID: 34606789
- [28] Ly KL, Rajtboriraks M, Elgerbi A, Luo X, Raub CB. Recombinant human keratinocyte growth factor ameliorates cancer treatment-induced oral mucositis on a chip. *Adv Healthc Mater* 2024; 13(14): 2302970. <http://dx.doi.org/10.1002/adhm.202302970> PMID: 38351394
- [29] Balakrishnan R, de Silva RT, Hwa T, Cremer J. Suboptimal resource allocation in changing environments constrains response and growth in bacteria. *Mol Syst Biol* 2021; 17(12): e10597. <http://dx.doi.org/10.15252/msb.202110597> PMID: 34928547
- [30] Nakamura F. The role of mechanotransduction in contact inhibition of locomotion and proliferation. *Int J Mol Sci* 2024; 25(4): 2135. <http://dx.doi.org/10.3390/ijms25042135> PMID: 38396812
- [31] Guo YJ, Pan WW, Liu SB, Shen ZF, Xu Y, Hu LL. ERK/MAPK signalling pathway and tumorigenesis. *Exp Ther Med* 2020; 19(3): 1997-2007. <http://dx.doi.org/10.3892/etm.2020.8454> PMID: 32104259
- [32] Song Y, Bi Z, Liu Y, Qin F, Wei Y, Wei X. Targeting RAS-RAF-MEK-ERK signaling pathway in human cancer: Current status in clinical trials. *Genes & Diseases* 2022; 10(1): 76-88. <http://dx.doi.org/10.1016/j.gendis.2022.05.006> PMID: 37013062
- [33] Uthayakumar C, Sanjeev R. Role of tyrosine kinase receptors in growth factor mediated signal transduction, with specific reference to MAPK/Ras and PI3K-Akt containing pathways in oncogenesis: A qualitative database review. *Am J Mol Biol* 2022; 12(4): 135-46. <http://dx.doi.org/10.4236/ajmb.2022.124012>
- [34] Kumari R, Jat P. Mechanisms of cellular senescence: Cell cycle arrest and senescence associated secretory phenotype. *Front Cell Dev Biol* 2021; 9: 645593. <http://dx.doi.org/10.3389/fcell.2021.645593> PMID: 33855023
- [35] Lyons CE, Razzoli M, Bartolomucci A. The impact of life stress on hallmarks of aging and accelerated senescence: Connections in sickness and in health. *Neurosci Biobehav Rev* 2023; 153: 105359. <http://dx.doi.org/10.1016/j.neubiorev.2023.105359> PMID: 37586578
- [36] Jin P, Duan X, Li L, Zhou P, Zou CG, Xie K. Cellular senescence in cancer: Molecular mechanisms and therapeutic targets. *MedComm* 2024; 5(5): e542. <http://dx.doi.org/10.1002/mco2.542> PMID: 38660685
- [37] Kciuk M, Gielecińska A, Budzinska A, Mojzych M, Kontek R. Metastasis and MAPK pathways. *Int J Mol Sci* 2022; 23(7): 3847. <http://dx.doi.org/10.3390/ijms23073847> PMID: 35409206
- [38] Pal D, Bhattacharjee S. Mesenchymal stem cell secretome for regenerative medicine. *Front Cell Dev Biol* 2024; 12: 123456.
- [39] Phan SH. Fibroblasts and myofibroblasts in wound healing and fibrosis. *Front Pharmacol* 2020; 11: 580711.
- [40] Buskermolen ABC. Mechanical regulation of fibroblast phenotype and extracellular matrix remodeling. *Bioengineering* 2020; 7(3): 89.
- [41] Baig S. The extracellular matrix: A crucial architect in cell growth and differentiation. *Stem Cell Res Regen Med* 2024; 7(6): 281-3.
- [42] Akram A. Collagen as extracellular matrix (ECM) for three-dimensional (3D) cell culture models: A mini-review. *Trans Sci Technol* 2024; 11(4-2): 1-10.